A&A 508, 833–839 (2009)
DOI: 10.1051/0004-6361/200911736

Astronomy & Astrophysics

Search for associations containing young stars (SACY)

III. Ages and Li abundances⋆,⋆⋆

L. da Silva[1], C. A. O. Torres[2], R. de la Reza[1], G. R. Quast[2], C. H. F. Melo[3], and M. F. Sterzik[3]

[1] Observatório Nacional-MCT, Rio de Janeiro, Brazil
e-mail: licio@on.br
[2] Laboratório Nacional de Astrofísica-MCT, Itajubá, Brazil
[3] European Southern Observatory, Alonso de Cordova 3107, Casilla 19, Santiago, Chile

Received 27 January 2009 / Accepted 28 August 2009

ABSTRACT

Context. Our study is a follow-up of the SACY project, an extended high spectral resolution survey of more than two thousand optical counterparts to X-ray sources in the southern hemisphere targeted to search for young nearby association. Nine associations have either been newly identified, or have had their member list revised. Groups belonging to the Sco-Cen-Oph complex are not considered in the present study.
Aims. These nine associations, with ages of between about 6 Myr and 70 Myr, form an excellent sample to study the Li depletion in the pre-main sequence (PMS) evolution. In the present paper, we investigate the use of Li abundances as an independent clock to constrain the PMS evolution.
Methods. Using our measurements of the equivalent widths of the Li resonance line and assuming fixed metallicities and microturbulence, we calculated the LTE Li abundances for 376 members of various young associations. In addition, we considered the effects of their projected stellar rotation.
Results. We present the Li depletion as a function of age in the first hundred million years for the first time for the most extended sample of Li abundances in young stellar associations.
Conclusions. A clear Li depletion can be measured in the temperature range from 5000 K to 3500 K for the age span covered by the nine associations studied in this paper. The age sequence based on the Li-clock agrees well with the isochronal ages, the ϵCha association being the only possible exception. The lithium depletion patterns for the associations presented here resemble those of the young open clusters with similar ages, strengthening the notion that the members proposed for these loose young associations have indeed a common physical origin. The observed scatter in the Li abundances hampers the use of Li in determining reliable ages for individual stars. For velocities above 20 km s^{-1}, rotation seems to play an important role in inhibiting the Li depletion.

Key words. stars: abundances – stars: pre-main sequence – stars: late-type – star: evolution

1. Introduction

In Torres et al. (2006) (hereafter Paper I) we report the results of a high-resolution optical spectroscopic survey to search for associations containing young stars (SACY) among optical counterparts of ROSAT All-Sky X-ray sources in the southern hemisphere. There we present the catalog resulting from the survey. We describe the convergence method developed to search for members of an association and a corresponding membership probability model. A membership to an association is defined in the hexa-dimensional space formed by the (UVW) velocity space and the (XYZ) spatial coordinates distribution. We also take into account the position in the HR diagram, eliminating very discrepant stars. Finally, we check each member proposed by comparing its Li content with the Li distribution of the association. The β Pictoris association (βPA) is presented as an example of the method outlined in Paper I.

In Paper I, we also present the Li abundance analysis of the βPA to confirm its youth. In contrast to open clusters where Li abundances have been studied over more than one decade (see Pallavicini et al. 2000), the results of Paper I was the first analysis of this kind for a young association.

Using the method described in Paper I, Torres et al. (2008, hereafter TQMS08) defined nine new young associations, namely, ϵ Chamaleontis (ϵChA), TW Hydrae (TWA), β Pictoris, Octants (OctA), Tucana-Horologium (THA), Columba (ColA), Carina (CarA), Argus (ArgA), and AB Doradus (ABDA). The present work continues this study and aims to derive the distribution of Li abundances for each of the nine associations resulting from a consolidated list of members. Since these associations are young, covering ages from about 5 Myr up to that of the Pleiades, they form an interesting "laboratory" for studying the Li depletion with age, as achieved for some open clusters (Randich et al. 2001; Jeffries 2006).

2. Sample

In Table 1, we present some properties of the young associations studied in this paper derived in TQMS08. The number of members (N), the number of Li eliminated stars ("intruders", n), the average distance (in parsecs), and the age (in Myr) taken from TQMS08 are given in Table 1. Li abundances were measured

⋆ Based on observations collected at the ESO – La Silla and at the LNA-OPD.
⋆⋆ Tables 3–11 are only available in electronic form at http://www.aanda.org

Table 1. Properties of the associations studied in this paper.

Association	N	n	distance	Age
ϵ Chamaleontis (ϵChA)	23	0	93–123	6
TW Hydrae (TWA)	22	0	28–73	8
β Pictoris (βPA)	48	2	10–80	10
Octans (OctA)	15	0	82–175	20?
Tucana-Horologium (THA)	45	1	37–78	30
Columba (ColA)	44	0	35–150	30
Carina (CarA)	23	1	45–160	30
Argus (ArgA)	64	1	29–164	40
AB Doradus (ABDA)	92	4	7–143	70

for 376 stars. Although the data are mainly from Paper I, a few additional data obtained since then are included and will be published in forthcoming papers.

These new observations allowed us to refine the definitions of some of the associations. For the ColA, we are able to obtain a similar but more consistent solution with a few changes to the member list with respect to those of TQMS08 (three stars now being rejected and six new ones included).

For the ABDA, three new members have been proposed, one of them, HD 82879, previously proposed to be a member of the ϵChA. Proposed by Zuckerman & Song (2004) as a member of the THA, HD 53842 was previously rejected in TQMS08 as a member of THA because of a compilation error. Its reintroduction now as a member proposed for the THA has no other consequences for the mean values of this association[1].

As explained in TQMS08, IC 2391 members were incorporated into the ArgA member list. Similarly, members of the open cluster η Cha were combined with the ϵChA members forming a unique group. The link between young loose associations and some open clusters will be discussed in forthcoming papers.

3. Li abundance determinations

The observations were carried out using the FEROS spectrograph (Kaufer et al. 1999) at la Silla, ESO, and the Coudé spectrograph of the 1.62 m telescope of the Observatório do Pico dos Dias, LNA, Brazil (see Paper I for details). The Li abundances ($A_{\rm Li}$) of the stars, in dex, in the system $\log A({\rm H}) = 12$, where A(H) is the H abundance ($A_{\rm Li} = \log N({\rm Li})/N({\rm H}) + 12$), were determined using the programs of M. Spite, of the Paris-Meudon Observatory. Our method is similar to that used for the βPA in Paper I. The main difference is that we now apply the atmospheric models of Kurucz and Castelli[2] instead of those of Gustafsson et al. (1975) used in Paper I.

The $A_{\rm Li}$ were determined from the resonance line at λ 6708. The method consists of calculating theoretical equivalent widths of the Li line ($EW_{\rm Li}$) and comparing them with their corresponding observed values. The $A_{\rm Li}$ is changed until the difference between the calculated and the observed $EW_{\rm Li}$ is smaller than 0.2 mÅ. The line was considered to be formed only by the ^{7}Li isotope. In the computation of the synthetic profile, we take into account the four components of the ^{7}Li resonance line, i.e., the wavelengths and the oscillators strengths given by Andersen et al. (1984), at wavelengths

[1] With these updates of the THA and the ColA, only 11 of the 50 stars listed by Zuckerman & Song (2004) are not found by us as high probability members of one of the GAYA associations (see Sect. 3 of Torres et al. 2008).

[2] http://www.user.oat.ts.astro.it/castelli

Table 2. Variation in Li abundance as a function of EW and model parameters.

Parameter	change	$\Delta A({\rm Li})_1$	$\Delta A({\rm Li})_2$
$T_{\rm eff}$[K]	±100	$^{+0.18}_{-0.19}$	$^{+0.08}_{-0.07}$
$\log g$	±0.5	$^{+0.16}_{-0.11}$	$^{+0.12}_{-0.06}$
microturbulence [km s^{-1}]	±0.5	$^{+0.05}_{-0.05}$	$^{+0.02}_{-0.02}$
EW	±10%	$^{+0.04}_{-0.05}$	$^{+0.05}_{-0.05}$
[Fe/H]	±0.1	$^{-0.03}_{+0.04}$	$^{-0.01}_{+0.02}$

λ 6707.754, λ 6707.766, λ 6707.904, λ 6707.917; and for $\log gf$: −0.430, −0.209, −0.733, −0.510, respectively.

Effective temperatures were obtained from the photometric and spectroscopic data available. The calibrations used were mainly those of Kenyon & Hartmann (1995) and Schmidt-Kaler (1982). Some additional information was included from Bessell (1979) and from Ducati et al. (2001). If a reliable Cousins $(V-I)_{\rm c}$ color index was available, either from our observations, from Hipparcos, or from other sources in the literature, this was used to derive $T_{\rm eff}$. In the absence of $(V-I)_{\rm c}$, we used the Johnson $(B-V)$, mainly derived from TYCHO-2 but also obtained from various sources in the literature. We considered the $(B-V)$ colors from TYCHO-2 reliable only for stars brighter than magnitude 10. Finally, if no reliable photometry was available, we used the spectral type to obtain the effective temperature.

The other model parameters were kept fixed: metallicity at [Fe/H] = 0.1 (see Castilho et al. 2005); and surface gravity $\log g$ was fixed at 4.5 for the dwarfs, and at 4.0 for the subgiants, according to the spectral classification of Paper I. The microturbulence velocity was fixed at 1.5 km s^{-1} for all stars.

3.1. Error analysis

Table 2 summarizes the internal errors expected in the Li abundances as a function of the variations in the model parameters and in the equivalent width. $\Delta A({\rm Li})_1$ and $\Delta A({\rm Li})_2$ are the Li abundances variations for a star with an effective temperature of 4000 K and 6100 K, respectively. Our main error source is the effective temperature. The unknown parameters, i.e., [Fe/H] and the microturbulence velocity, are less important, and the values used are good estimates. The small sensitivity of the Li abundance to the microturbulence velocity may be surprising, but it may be because the fine structure of the Li line is used and each line component is a weak line, thus not making very significant contribution to the microturbulence velocity. An error of 10% in the EW is perhaps optimistic for the weak lines. An increase in the error of the EW to 20% results in a variation of $A_{\rm Li}$ of 0.08 at $T_{\rm eff}$ = 4000 K and of 0.09 at 6100 K. From Table 2, we can say that our internal errors are smaller than 0.2, sufficient to reach our goal. As can be seen from our abundance results in the figures, even a difference as high as 0.2 does not modify any of our conclusions.

How does the choice of different models change our results? In order to address this question, we compare our results using Kurucz models with those using the Uppsala group models, which were used in Paper I. Using atmospheric models calculated with the MARCS code, developed by the Uppsala group[3] (see Gustafsson et al. 1975), we obtain a value of $A_{\rm Li}$ that is 0.09 larger at 4000 K than using Kurucz models. At 6000 K,

[3] http://marcs.astro.uu.se/

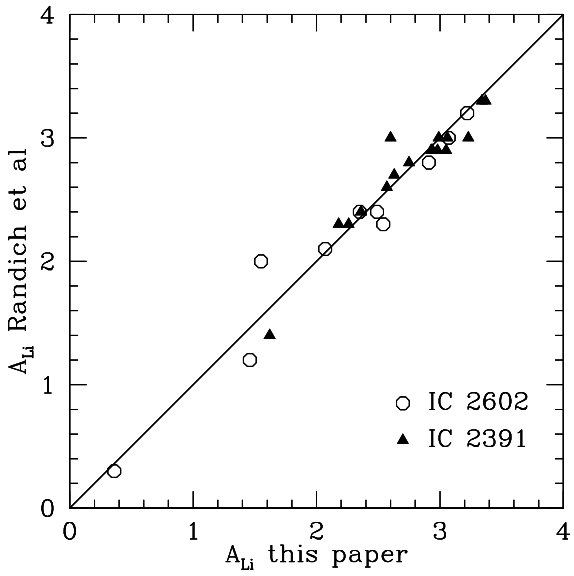

Fig. 1. Comparison between our results and those of Randich et al. (2001) for the stars in IC 2391 and IC 2602.

the difference is 0.07, in the same direction. For homogeneity purposes, we used Kurucz models in our analysis because they begin at 3500 K, whereas MARCS models begin only at 4000 K. Nevertheless, this shows how sensitive the use of different $A_{\rm Li}$ values from different authors can be. In this case, the difference between our $A_{\rm Li}$ results and those of other authors could even be larger than 0.2, which we adopt as our internal error.

As an additional test, we compared our abundances for IC 2391 (considered to be ArgA members) with those from Randich et al. (2001). Using the *EW* from these authors, we also computed the Li abundances for the IC 2602 members as described above. The agreement between both Li abundances is very good (Fig. 1) validating our method.

4. Results and discussion

Table 1 summarizes some properties given in TQMS08 for the nine young associations. This table contains the proposed ages, the most important parameter for our Li evolution study. Distance is a rather meaningless quantity for these nearby associations (due to their proximity their members have a wide range of distances). The Li abundances determined for all high probability members, in all 376 stars, are given in Tables 4 to 12. The tables contain the identifications of the members of each association, their coordinates, the $EW_{\rm Li}$, the $T_{\rm eff}$, the $A_{\rm Li}$, and the projected stellar rotational velocities ($v \sin(i)$). More details about the association memberships can be found in TQMS08.

Stars cooler than 3500 K are not covered by the Kurucz models and are given here for reference only. Those values are calculated with extrapolated models, and they have errors potentially larger than those considered above. Those objects have not been considered in our figures and discussion.

4.1. Lithium depletion pattern and open cluster ages

The lithium depletion pattern (LDP) for all nine young associations studied in this paper is shown in Fig. 2. For each association, stars were divided into two groups according to their $v \sin(i)$. Stars rotating slower than 20 km s^{-1} are shown as open squares, whereas those rotating faster than 20 km s^{-1} are marked as filled circles. Stars whose $v \sin i$ could not be determined are plotted as crosses. Along with the derived abundances and effective temperatures, a 4th-degree polynomial fit of the data is shown as a solid line. This line defines the LDP of each association.

Using the data from Sestito & Randich (2005), we computed the LDPs for the young clusters studied by these authors and compared with those LPDs of the young associations at similar ages.

In the top panel of Fig. 4, we show the Li abundances for IC 2391 and IC 2602, which both have an age similar to that of THA (30 Myr). The LDP of THA is shown as a thick black line, whereas the LDP obtained for these two young clusters are seen as a thick dashed black line. For comparison, the LPD for βPA (10 Myr) and ABDA (70 Myr) are shown as light solid and dashed light line, respectively.

In the middle panel of Fig. 4, the Li abundance for α Per and NGC 2451 (50 Myr) are plotted. In this case, the LDP shown as a thick, solid line is that of ArgA. Solid and dashed light lines again represent the LDPs for βPA and ABDA. Finally, the Li abundances for the Pleiades members are shown in the bottom panel of Fig. 4. The thick black line is the LDP of ABDA. The βPA LDP is again shown as a solid light, line along with the LDP of THA shown as a light, dashed line.

Despite the dispersion in the observational data, the agreement between the LDPs of the young clusters and those of the young association is reasonably good. An exception are the data for α Per and NGC 2451, which show a level of Li depletion close to that of the Pleiades. According to the LDP of the ArgA, abundances ~0.5 dex higher were expected.

Although the comparison with the young clusters remains marginal (due to the low number of clusters and high dispersion), the good agreement found is already an important result. First, it provides confidence in our derivation of the Li abundances described in Sect. 3. Secondly, that the LDP of the nine associations are similar to the LDP of open clusters of similar ages strengthens the notion that the associations presented in TQMS08 are indeed physical groups of stars sharing a common formation history.

4.2. Lithium depletion pattern and the relative ages

All observational LDPs (i.e., the polynomial fits to the observed Li abundances as a function of $T_{\rm eff}$ shown in Fig. 2) have been plotted together in the left panel of Fig. 3. LDPs for each association are identified by its line style and marker type (see caption of Fig. 3).

As expected, Li abundances for stars with temperatures hotter than about 5000 K are almost constant over the time span (~65 Myr) covered by our sample of associations (King 1998; Soderblom et al. 1999; Randich et al. 1997, 2001; Stauffer et al. 1989; Martin & Montes 1997; Jeffries et al. 2003; Balachandran et al. 1988, 1996; Randich et al. 1998; Martín 1997). On the other hand, for those associations possessing members with effective temperatures as low as to 3600 K, the observed LDPs are clearly distinguishable (right panel of Fig. 3).

A closer look into these different lines in the right panel and into the ages quoted in Table 1 shows that there is indeed a gradual shift in the cool end of the observed LDP as a function of age. The age sequence seen in Fig. 3 matches that proposed in TQMS08 based on an isochronal fit of the color−magnitude diagram restricted to the G- and K-type stars (see TQMS08 for details). The only exception is the ϵChA, which seems to be older according to its LDP. Given the isochronal age of 6 Myr

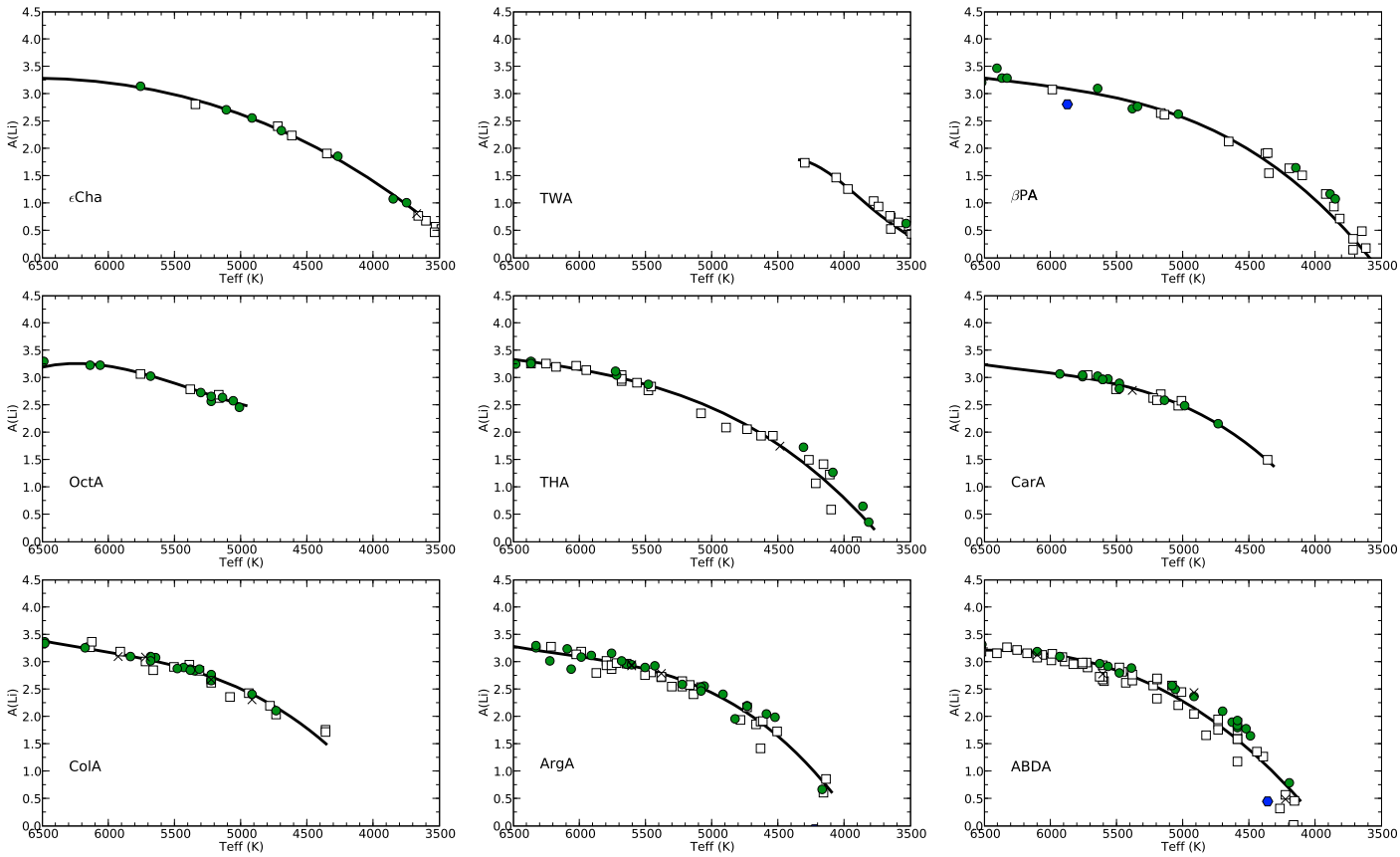

Fig. 2. Lithium depletion pattern for all nine associations presented in this paper. Plots are arranged in the age sequence of Table 1. Stars rotating slower (faster) than 20 km s^{-1} are shown as open squares (filled circles). Stars whose $v \sin i$ could not be determined are plotted as crosses. Filled hexagons are Li intruders. A 4th-degree polynomial fit of the data is shown as a solid line.

derived in Paper II, one would expect a flat LDP around the cosmic Li abundance of A(Li) = 3.1, as found in T-Tauri stars (e.g., Martin et al. 1994) and young clusters (e.g., Palla et al. 2005; Zapatero Osorio et al. 2002). That a Li depletion is seen might indicate that ϵ Cha could be a bit older. This is discussed below in Sect. 4.3.

The three associations with 30 Myr, namely, THA, CarA, and ColA were suggested in TQMS08 to be structures of the Great Austral Young Association (GAYA) complex. From the Li abundance point of view, these three groups are indistinguishable indicating that indeed they have very similar ages in agreement with the suggestion of TQMS08.

From Fig. 2, it is clear that there is an important scatter around the mean LDP for any given associations. This scatter is real and not a consequence of the errors. For example, the stars HD 6569, HIP 26401B, and UY Pic, all members of the ABDA (that is, with the same age and metallicity) have all high quality observations, similar values of both $T_{\rm eff}$ (therefore similar masses) and $v \sin(i)$ (10, 5 and 9 km s^{-1}). However, they have very different $A_{\rm Li}$ values, respectively 2.28, 3.32, and 3.66.

The bottom line is that a distinct Li depletion history causes a significant scatter in the observed LDP preventing the use of Li as a clock for dating individual stars. However, statistically speaking, Li abundances derived in a homogeneous way as done in this paper can be used to determine relative ages of the young associations provided that the associations possess enough members cooler than 5000−4500 K. Our conclusions are similar to those of Mentuch et al. (2008), who also found qualitatively good agreement between the Li abundances and the isochronal ages of a small number of stars belonging to the five associations studied here.

As for the Li "intruders", only two stars (HD 190102 in the βPA, and CD-41 2076 in the ABDA) out of the nine rejected as members of the associations proposed in TQMS08 based on their low Li abundance, have A(Li) values relatively close to the LDP of their associations. They are shown as filled hexagons in Fig. 2. The other intruders are shown only in Tables 4−12. HD 190102 was rejected because its Li is too low even if the typical scatter in the Li abundance of the βPA members is considered. CD-41 2076, which has a Li that is still acceptable for the ABDA, lies 1.1 mag above its isochrone. For either of these two objects to be reconciled as a bonafide member, their photometric magnitudes (from TYCHO-2) must have a large error and/or they must be an unresolved binary. In this last case probably the Li abundance could have been underestimated. We found no indication of the presence of a companion around these two objects. In any case, these two examples show that we must act with caution when eliminating stars based only on Li abundances.

4.3. The age of the ϵCha association

The age estimated in TQMS08 for the ϵChA is 6 Myr, which is within the range of 3−15 Myr found in the literature (Fernández et al. 2008; Terranegra et al. 1999; Jilinski et al. 2005; Feigelson et al. 2003). We should bear in mind that a given association might have a different member list according to the method and criteria used to define it. Therefore, ages determined by different methods are not always trivial to be compared.

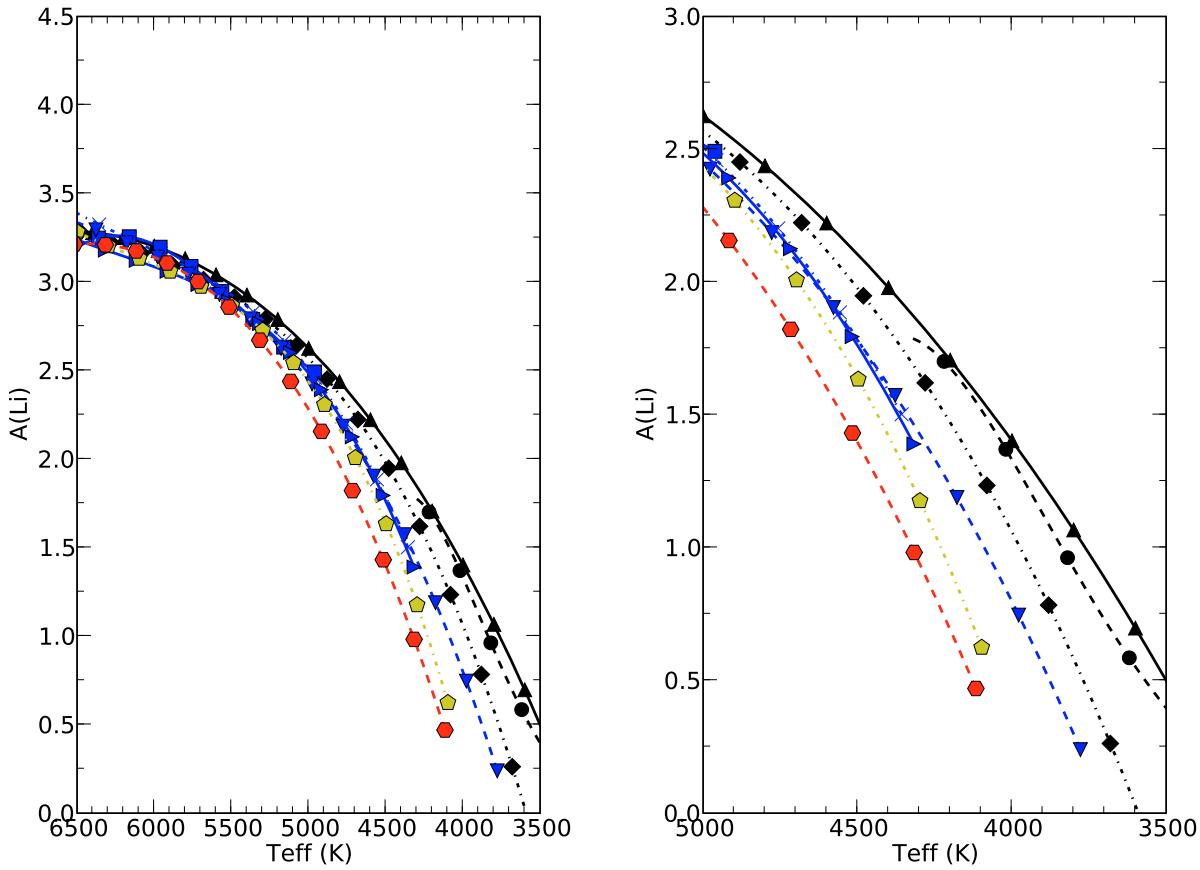

Fig. 3. Comparison of the polynomial fit of the observed LDPs. *Left*. All polynomial fits for the associations shown in Fig. 2. For each association, LDPs are identified by a line type and a symbol as follow: ϵChaA (solid line, filled triangles), TWA (dashed line, filled circles), βPicA (dotted line, diamonds), OctA (solid line, square), THA (dashed line, downwards triangle), ColA (dashed-dotted line, crosses), CarA (solid line, rightwards triangle), ArgA (dashed-dotted, pentagon), and ABDA (dashed line, hexagon). The associations between 20−30 Myr are indistinguishable. *Right*. Zoom in $T_{\rm eff}$ cooler than 4800 K. At this region, a clear separation between the LDP is seen.

The Li abundances for NGC 2264 (5 Myr) show a flat distribution around A(Li) ∼ 3.2 for stars with 6500 K > $T_{\rm eff}$ > 4000 K, suggesting that no Li depletion has taken place (Sestito & Randich 2005; King 1998). Palla et al. (2005) see no depletion either for the bulk of Orion nebular cluster (ONC) (3 Myr) stars. The mean abundance is again 3.1−3.3. Undepleted lithium abundances were also reported by Zapatero Osorio et al. (2002) for the young σ Ori cluster. Based on theoretical predictions for the Li depletion, Zapatero Osorio et al. estimated the age of σ Ori to be around 2−4 Myr. It is worth noting that for the ONC and the σ Ori cluster, a small group of stars was found to show a considerable Li depletion with respect to the interstellar abundance. The observed depletion in the Li content was explained by Palla et al. (2005) for the ONC and by Sacco et al. (2007) for σ Ori as a result of an age spread within those two clusters.

Our Fig. 3 indeed supports the idea that the age of the ϵChaA is at least as young as the TWA but older than that of NGC 2264, ONC and, the σ Ori cluster and certainly younger than the βPA.

4.4. Li and rotation

A careful inspection of Fig. 2 shows that stars rotating faster than 20 km s^{-1} (filled circles) are often above the polynomial fit of the LDP of the associations, suggesting that already at this level, rotation might play a role in the Li depletion.

This is more clearly seen in Fig. 7, where the histograms of the differences between the derived abundances and the polynomial fit of the observed LDP is shown for rotations slower and faster than 20 km s^{-1}.

Addressing the role of rotation using $V \sin i$ might lead to erroneous conclusions since the true rotation of the star is unknown because of the $\sin i$ factor. As an example, we compare in Fig. 6 the spectral region around the Li 6708 line for HD 6569 ($v \sin i$ = 10 km s^{-1}) and HIP 26401B ($v \sin i$ = 5 km s^{-1}). The CaI line at λ 6718, a good indicator of temperature (see Cutispoto et al. 1999), is also shown in the figure. The similarity of their Ca I lines confirms that both stars have very similar $T_{\rm eff}$, despite their obviously different Li line intensities.

We used the rotation-chromospheric flux relation derived by Noyes et al. (1984) using the Ca H & K lines ($R'_{\rm HK}$) to estimate the rotation period for both stars. The $R'_{\rm HK}$ were derived as described in Melo et al. (2006). The spectral region around the Ca H & K lines for both stars is shown in Fig. 5. The calibration of Melo et al. (2006) yields a $R'_{\rm HK}$ of −4.336 and −4.190, which translates into a rotation period of 7.2 days and 2.7 days for HD 6569 and HIP 26401B, respectively. According to the $R'_{\rm HK}$-$P_{\rm rot}$ calibration, HD 6569 rotates almost 3 times more slowly than HIP 26401B. Statistically speaking however, Fig. 7 is worth of mentioning since the true distribution of equatorial velocities computed from a deconvolution process does not differ considerably from the projected one (e.g., Royer et al. 2007).

There is a vast amount of literature showing that Li depletion is driven not only by convection, but that extra-mixing processes capable of inhibiting Li depletion during the PMS are also at

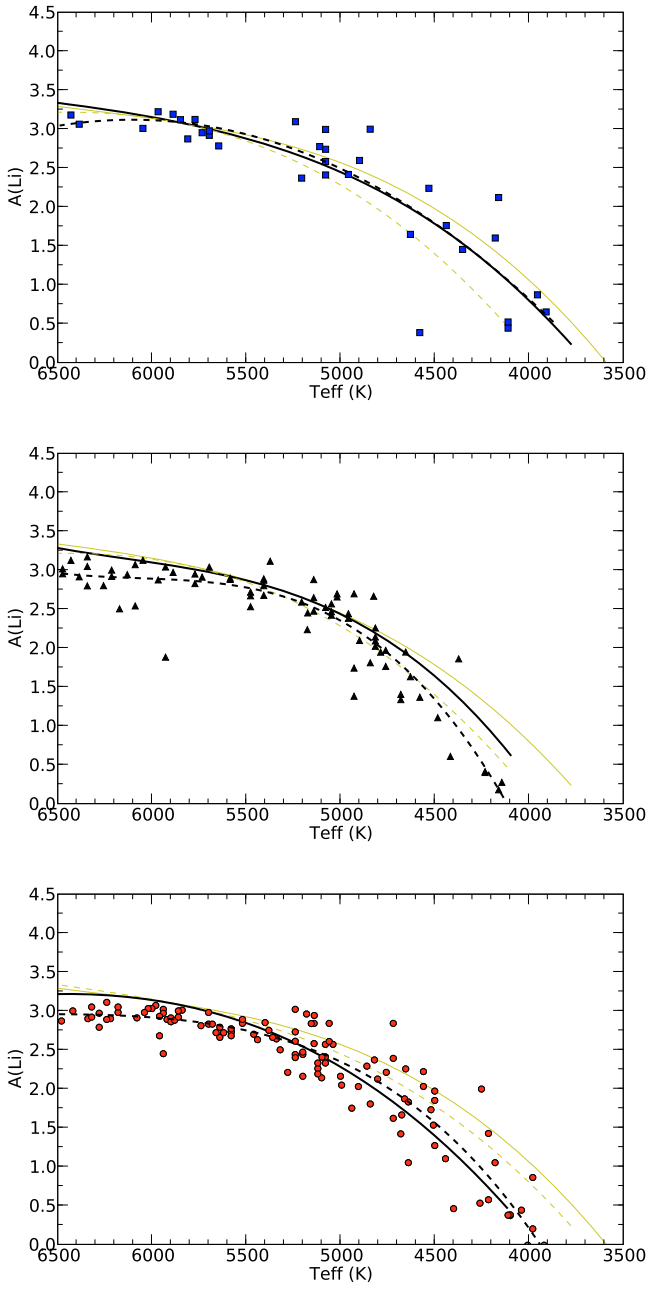

Fig. 4. Comparison between the LDPs of the young associations and the Li abundances for the young cluster (<100 Myr) from Sestito & Randich (2005). *Top*. IC 2602 and IC 2391, *Middle*. α Per and NGC 2451. *Bottom*. The Pleiades. For each panel our derived LDP having an age closest to that of the cluster is shown as thick black line (see text). The fitted LDP computed in the same way as for the young associations is shown as thick dashed black line.

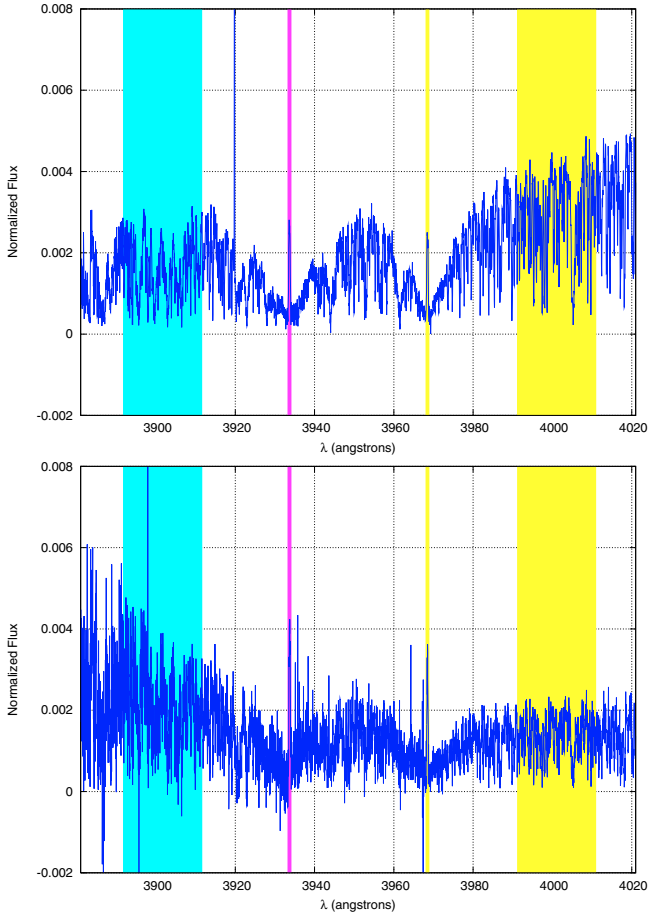

Fig. 5. Regions used to compute the CaII H & K flux. HD 6569 and HIP 26401B are shown in *the top and bottom panels*, respectively.

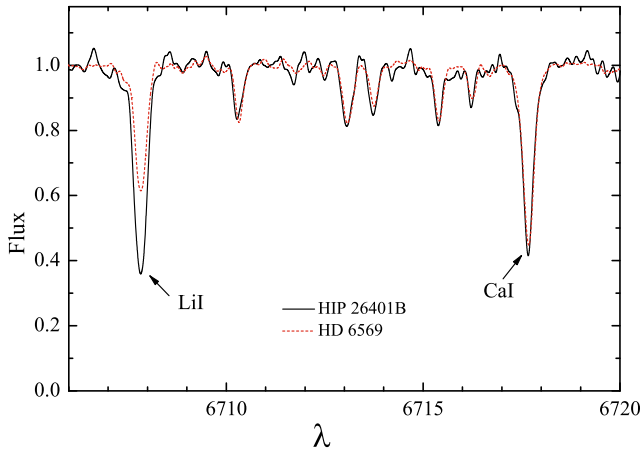

Fig. 6. Superposition of the spectra of the stars HD 6569 and HIP 26401B in the Li region. Both stars belong to the AB Doradus association and have the same $T_{\rm eff}$ – note the similarity between the CaI lines, a good temperature indicator – but have distinct Li line intensities.

work (e.g., Bouvier 2008; Deliyannis et al. 2000). The discussion of this complex issue is beyond the scope of this paper. Nevertheless, we point out that Fig. 7 indicates that a deeper look into the Li-rotation connection in this sample could be worthwhile.

5. Conclusions

We have completed a systematic study of the evolution of the Li abundances for the most extended sample of pre-main sequence stars belonging to young, loose, nearby associations. Nine associations with a total of 376 stars have been considered covering ages from ~5 Myr to almost that of the age of the Pleiades. Our results were compared to Li studies in young open clusters.

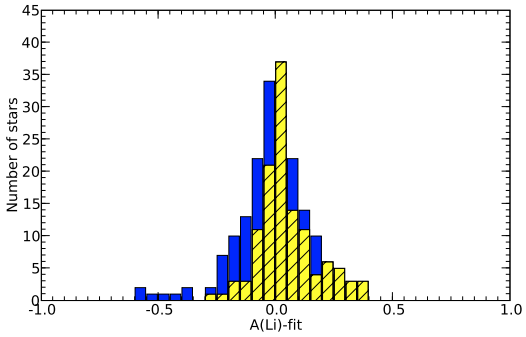

Fig. 7. Histogram of the differences between the derived abundances and the polynomial fit to the observed LDP. Dark gray and hatched light gray bins represent stars rotating slower and faster than 20 km s^{-1}, respectively.

Our main conclusions are the following:

- A clear Li depletion, considered as a measure of a systematic decrease in the Li abundance with age, can be measured in the temperature range from 5000 K to 3500 K for the age span covered by the nine associations studied in this paper.
- The age sequence based on the Li-clock agrees well with the isochronal ages of TQMS08.
- The ϵChA is the only possible exception with a LDP exhibiting a considerable Li depletion for late-type stars in comparison to young cluster of similar age.
- A true scatter in the Li abundance values, with variations larger than those originating in internal or systematic errors, is present. This scatter hampers the use of Li to determine reliable ages for individual stars.
- The Li depletion patterns for the associations presented here resemble those of young open clusters with similar ages, strengthening the notion that the stars of these loose associations have indeed a common physical origin.
- For velocities above 20 km s^{-1}, rotation seems to play an important role in inhibiting the Li depletion.

Acknowledgements. The authors wish to thank the staff of the Observatório do Pico dos Dias, LNA/MCT, Brazil and of the European Southern Observatory, La Silla, Chile. L.S. thanks the CNPq, Brazilian Agency, for the grant 301376/86-7. Sofia Randich is warmly thanked for sharing her Li data with us. We are grateful to the anonymous referee whose comments helped to improve the quality of the paper.

References

Andersen, J., Gustafsson, B., & Lambert, D. L. 1984, A&A, 136, 65
Balachandran, S., Lambert, D. L., & Stauffer, J. R. 1988, ApJ, 333, 267
Balachandran, S., Lambert, D. L., & Stauffer, J. R. 1996, ApJ, 470, 1243
Bessell, M. S. 1979, PASP, 91, 589
Bouvier, J. 2008, A&A, 489, L53
Castilho, B. V., Torres, C. A. O., Quast, G., et al. 2005, From Lithium to Uranium: Elemental Tracers of Early Cosmic Evolution, 228, 83
Cutispoto, G., Pastori, L., Tagliaferri, G., Messina, S., & Pallavicini, R. 1999, A&AS, 138, 87
Deliyannis, C. P., Pinsonneault, M. H., & Charbonnel, C. 2000, The Light Elements and their Evolution, Proc. IAU Symp., 198, 61
Ducati, J. R., Bevilacqua, C. M., Rembold, S. B., & Ribeiro, D. 2001, ApJ, 558, 309
Feigelson, E. D., Lawson, W. A., & Garmire, G. P. 2003, ApJ, 599, 1207
Fernández, D., Figueras, F., & Torra, J. 2008, A&A, 480, 735
González Hernández, J. I., Caballero, J. A., Rebolo, R., et al. 2008, A&A, 490, 1135
Gustafsson, B., Bell, R. A., Eriksson, K., & Nordlund, A. 1975, A&A, 42, 407
Hünsch, M., Randich, S., Hempel, M., Weidner, C., & Schmitt, J. H. M. M. 2004, A&A, 418, 539
Jeffries, R. D. 2006, Chemical Abundances and Mixing in Stars in the Milky Way and its Satellites, ESO Astrophys. Symp. (Springer-Verlag), 163, 163
Jeffries, R. D., Oliveira, J. M., Barrado y Navascués, D., & Stauffer, J. R. 2003, MNRAS, 343, 1271
Jilinski, E., Ortega, V. G., & de la Reza, R. 2005, ApJ, 619, 945
Kaufer, A., Stahl, O., Tubbesing, S., et al. 1999, The Messenger, 95, 8
Kenyon, S. J., & Hartmann, L. 1995, ApJS, 101, 117
King, J. R. 1998, AJ, 116, 254
Martín, E. L. 1997, Mem. Soc. Astron. It., 68, 905
Martin, E. L., & Montes, D. 1997, A&A, 318, 805
Martin, E. L., Rebolo, R., Magazzu, A., & Pavlenko, Y. V. 1994, A&A, 282, 503
Melo, C., Santos, N. C., Pont, F., et al. 2006, A&A, 460, 251
Mentuch, E., Brandeker, A., van Kerkwijk, M. H., Jayawardhana, R., & Hauschildt, P. H. 2008, ApJ, 689, 1127
Neuhäuser, R. 1997, Science, 276, 1363
Noyes, R. W., Hartmann, L. W., Baliunas, S. L., Duncan, D. K., & Vaughan, A. H. 1984, ApJ, 279, 763
Palla, F., Randich, S., Flaccomio, E., & Pallavicini, R. 2005, ApJ, 626, L49
Pallavicini, R., Randich, S., Stauffer, J. R., & Balachandran, S. C. 2000, The Light Elements and their Evolution, Proc. IAU Symp., 198, 350
Platais, I., Melo, C., Mermilliod, J.-C., et al. 2007, A&A, 461, 509
Randich, S., Aharpour, N., Pallavicini, R., Prosser, C. F., & Stauffer, J. R. 1997, A&A, 323, 86
Randich, S., Martin, E. L., Lopez, R. J. G., & Pallavicini, R. 1998, A&A, 333, 591
Randich, S., Pallavicini, R., Meola, G., Stauffer, J. R., & Balachandran, S. C. 2001, A&A, 372, 862
Royer, F., Zorec, J., & Gómez, A. E. 2007, A&A, 463, 671
Sacco, G. G., Randich, S., Franciosini, E., Pallavicini, R., & Palla, F. 2007, A&A, 462, L23
Sestito, P., & Randich, S. 2005, A&A, 442, 615
Schmidt-Kaler, T. 1982, in Landolt-Börnstein: Numerical Data and Functional Relationships in Science and Technology – New Series, VI/2b, ed. K. Schaifers, & H. H. Voigt (Springer-Verlag), 1
Siess, L., Dufour, E., & Forestini, M. 2000, A&A, 358, 593
Silva, W. P., & Silva, C. M. D. P. S. 2004, LAB Fit Ajuste de Curvas V.7.2.14e, online http://www.angelfire.com/rnb/labfit/index_p.htm
Soderblom, D. R., Jones, B. F., Balachandran, S., et al. 1993, AJ, 106, 1059
Soderblom, D. R., King, J. R., Siess, L., Jones, B. F., & Fischer, D. 1999, AJ, 118, 1301
Stauffer, J., Hartmann, L. W., Jones, B. F., & McNamara, B. R. 1989, ApJ, 342, 285
Terranegra, L., Morale, F., Spagna, A., Massone, G., & Lattanzi, M. G. 1999, A&A, 341, L79
Torres, C. A. O., Quast, G. R., da Silva, L., et al. 2006, A&A, 460, 695 (Paper I)
Torres, C. A. O., Quast, G. R., Melo, C. H. F., & Sterzik, M. F. 2008, Handbook of Star Forming Regions, Volume II, The Southern Sky ASP Monograph Publications, Vol. 5, ed. Bo Reipurth, 757 (TQMS08)
Zapatero Osorio, M. R., Béjar, V. J. S., Pavlenko, Y., et al. 2002, A&A, 384, 937
Zuckerman, B., & Song, I. 2004, ARA&A, 42, 685

Table 3. The β Pictoris association.

Ident	α(2000)	δ(2000)	$EW_{\rm Li}$ mÅ	$T_{\rm eff}$ K	$A_{\rm Li}$	$v \sin(i)$ km s^{-1}
HIP 10679	02 17 24.7	+28 44 30	160	5988	3.08	8
HD 14062	02 17 25.3	+28 44 42	140	6368	3.29	45
BD+30 397B	02 27 28.1	+30 58 41	110	3544	–0.19	
AG Tri	02 27 29.3	+30 58 25	220	4351	1.55	5
BD+05 378	02 41 25.9	+05 59 18	450	4100	1.51	9
HD 29391	04 37 36.1	–02 28 25		7555		95
GJ 3305	04 37 37.5	–02 29 28	120	3715	0.15	5
V1005 Ori	04 59 34.8	+01 47 01	270	3816	0.72	14
CD-57 1054	05 00 47.1	–57 15 25	360	3860	0.94	6
HIP 23418	05 01 58.8	+09 55 59	0	3496		8
BD-21 1074BC	05 06 49.5	–21 35 04	20	3496	–1.07	
BD-21 1074A	05 06 49.9	–21 35 09	20	3613	–0.88	
AF Lep	05 27 04.8	–11 54 03	191	6406	3.47	52
V1311 Ori	05 32 04.5	–03 05 29	100	3566	–0.20	12
β Pic	05 47 17.1	–51 03 59	0	8543		139
AO Men	06 18 28.2	–72 02 41	420	4377	1.91	16
HD 139084B	15 38 56.8	–57 42 19	460	3314	0.18	
V343 Nor	15 38 57.5	–57 42 27	292	5168	2.65	17
V824 Ara	17 17 25.5	–66 57 04	250	5383	2.73	31
HD 155555C	17 17 31.3	–66 57 06	20	3413	–1.17	6
GSC 8350-1924	17 29 20.7	–50 14 53	50	3480	–0.66	
CD-54 7336	17 29 55.1	–54 15 49	360	5036	2.63	35
HD 161460	17 48 33.7	–53 06 43	320	5140	2.62	10
HD 164249	18 03 03.4	–51 38 56	107	6597	3.31	22
HD 164249B	18 03 04.1	–51 38 56	70	3607	–0.30	
HD 165189	18 06 49.9	–43 25 31	0	7829		104
V4046 Sgr	18 14 10.5	–32 47 33	440	4361	1.92	14
GSC 7396-0759	18 14 22.1	–32 46 10	190	3619	0.18	3
HD 168210	18 19 52.2	–29 16 33	290	5645	3.10	115
HD 172555	18 45 26.9	–64 52 17	0	8323		116
CD-64 1208	18 45 36.9	–64 51 48	490	4148	1.65	110
TYC 9073-0762-1	18 46 52.6	–62 10 36	332	3649	0.49	10
CD-31 16041	18 50 44.5	–31 47 47	492	3889	1.17	50
PZ Tel	18 53 05.9	–50 10 50	287	5344	2.77	69
TYC 6872-1011-1	18 58 04.2	–29 53 05	483	3850	1.08	34
CD-26 13904	19 11 44.7	–26 04 09	320	4655	2.13	10
η Tel	19 22 51.2	–54 25 26	0	9670		330
HD 181327	19 22 58.9	–54 32 17	120	6597	3.36	21
HD 191089	20 09 05.2	–26 13 26	95	6521	3.21	45
AT MicB	20 41 51.1	–32 26 10	0	3331		16
AT MicA	20 41 51.2	–32 26 07	0	3341		10
AU Mic	20 45 09.5	–31 20 27	80	3649	–0.16	9
HD 199143	20 55 47.7	–17 06 51	147	6330	3.29	129
AZ Cap	20 56 02.7	–17 10 54	420	4197	1.64	16
CP-72 2713	22 42 48.9	–71 42 21	440	3921	1.17	8
WW PsA	22 44 58.0	–33 15 02	0	3391		12
TX PsA	22 45 00.0	–33 15 26	450	3316	–0.09	17
BD-13 6424	23 32 30.9	–12 15 52	185	3715	0.35	9
		Intruders				
HD 190102	20 04 18.1	–26 19 46	110	5874	2.82	
TYC 9114-1267-1	21 21 28.7	–66 55 06	15	3889	–0.47	4

Table 4. The Tucana-Horologium association.

Ident	α(2000)	δ(2000)	$EW_{\rm Li}$ mÅ	$T_{\rm eff}$ K	$A_{\rm Li}$	$v \sin(i)$ km s^{-1}
HD 105	00 05 52.5	–41 45 11	153	6178	3.20	14
HD 987	00 13 53.0	–74 41 18	202	5481	2.77	7
HD 1466	00 18 26.1	–63 28 39	130	6368	3.26	18
HIP 1910	00 24 09.0	–62 11 04	194	3860	0.65	21
CT Tuc	00 25 14.7	–61 30 48	40	3841	–0.13	7
HD 2884	00 31 32.7	–62 57 30	0	9670		107
HD 2885	00 31 33.5	–62 57 56	18	9036	3.90	6
HD 3003	00 32 43.9	–63 01 53	0	9146		78
HD 3221	00 34 51.2	–61 54 58	360	4309	1.73	123
CD-78 24	00 42 20.3	–77 47 40	291	4540	1.94	19
HD 8558	01 23 21.3	–57 28 51	196	5683	2.94	14
CC Phe	01 28 08.7	–52 38 19	168	4894	2.09	3
DK Cet	01 57 49.0	–21 54 05	190	5950	3.14	15
HD 13183	02 07 18.1	–53 11 56	229	5721	3.05	24
HD 13246	02 07 26.1	–59 40 46	141	6368	3.30	36
CD-60 416	02 07 32.2	–59 40 21	254	4268	1.50	11
ϕ Eri	02 16 30.6	–51 30 44	0	15665		240
ϵ Hyi	02 39 35.4	–68 16 01	0	10852		96
CD-53 544	02 41 46.8	–52 59 52	298	4087	1.27	80
AF Hor	02 41 47.3	–52 59 31	10	3511	–1.35	10
CD-58 553	02 42 33.0	–57 39 37	120	4216	1.07	6
CD-35 1167	03 19 08.7	–35 07 00	65	4100	0.59	6
CD-46 1064	03 30 49.1	–45 55 57	229	4487	1.75	
CD-44 1173	03 31 55.7	–43 59 14	251	4110	1.23	11
HD 22213	03 34 16.4	–12 04 07	260	5729	3.12	42
HD 22705	03 36 53.4	–49 57 29	154	6254	3.26	18
BD-12 943	04 36 47.1	–12 09 21	240	5460	2.84	17
HD 29615	04 38 43.9	–27 02 02	200	6026	3.22	18
HD 30051	04 43 17.2	–23 37 42	120	6798	3.44	
TYC 8083-0455-1	04 48 00.7	–50 41 26	40	3908	0.01	5
HD 32195	04 48 05.2	–80 46 45	130	6368	3.26	41
BD-20 951	04 52 49.5	–19 55 02	190	5083	2.35	
BD-19 1062	04 59 32.0	–19 17 42	230	4735	2.06	12
BD-09 1108	05 15 36.5	–09 30 51	245	5683	3.05	18
CD-30 2310	05 18 29.0	–30 01 32	310	4158	1.42	7
HD 53842	06 46 13.5	–83 59 30		6597		
α Pav	20 25 38.9	–56 44 06	0	17726		35
HD 202917	21 20 50.0	–53 02 03	227	5567	2.91	15
HIP 107345	21 44 30.1	–60 58 39	55	3824	–0.01	8
HD 207575	21 52 09.7	–62 03 09	110	6483	3.25	30
HD 207964	21 55 11.4	–61 53 12	100	7006	3.48	110
TYC 9344-0293-1	23 26 10.7	–73 23 50	123	3816	0.36	61
CD-86 147	23 27 49.4	–86 13 19	276	5481	2.88	74
HD 222259B	23 39 39.3	–69 11 40	232	4629	1.94	15
DS Tuc	23 39 39.5	–69 11 45	216	5683	2.98	18
		Intruders				
CD-34 521	01 22 04.4	–33 37 04	0	4226		5

Table 5. The Columba association.

Ident	α(2000)	δ(2000)	$EW_{\rm Li}$ mÅ	$T_{\rm eff}$ K	$A_{\rm Li}$	$v \sin(i)$ km s^{-1}
BD-16 351	02 01 35.6	–16 10 01	190	5083	2.36	9
BD-11 648	03 21 49.7	–10 52 18	320	5225	2.77	27
V1221 Tau	03 28 15.0	+04 09 48	275	5645	3.08	96
HD 21955	03 31 20.8	–30 30 59	230	5835	3.10	22
HD 21997	03 31 53.6	–25 36 51	0	8707		70
BD-04 700	03 57 37.2	–04 16 16	250	5506	2.91	14
BD-15 705	04 02 16.5	–15 21 30	220	4735	2.04	7
HD 26980	04 14 22.6	–38 19 02	183	6140	3.27	14
HD 27679	04 21 10.3	–24 32 21	180	5928	3.10	
CD-43 1395	04 21 48.7	–43 17 33	270	5683	3.10	26
CD-36 1785	04 34 50.8	–35 47 21	300	4941	2.43	9
BD+08 742	04 42 32.1	+09 06 01	240	5225	2.62	14
HD 30447	04 46 49.5	–26 18 09		6897		70
GSC 8077-1788	04 51 53.0	–46 47 31	30	3655	–0.62	
HD 31242	04 51 53.5	–46 47 13	250	5721	3.09	
HD 272836	04 53 05.2	–48 44 39	250	4917	2.31	
TYC 5900-1180-1	04 58 35.8	–15 37 31	290	5383	2.87	40
BD-08 995	04 58 48.6	–08 43 40	270	5225	2.68	7
HD 32372	05 00 51.9	–41 01 07	210	5721	3.01	8
AS Col	05 20 38.0	–39 45 18	140	6483	3.37	72
BD-08 1115	05 24 37.3	–08 42 02	280	5432	2.90	33
HD 35841	05 26 36.6	–22 29 24		6556		
HD 274561	05 28 55.1	–45 34 58	270	4781	2.20	7
HD 36329	05 29 24.1	–34 30 56	220	5912	3.19	8
AG Lep	05 30 19.1	–19 16 32	230	5683	3.02	21
HD 37484	05 37 39.6	–28 37 35	125	6848	3.53	43
TYC 0119-1242-1	05 37 45.3	+02 30 57	330	4361	1.76	10
TYC 0119-0497-1	05 37 46.5	+02 31 26	300	4361	1.72	13
BD-08 1195	05 38 35.0	–08 56 40	290	5352	2.84	29
HD 38207	05 43 21.0	–20 11 21		6656		
HD 38206	05 43 21.7	–18 33 27	0	9366		41
CD-38 2198	05 45 16.3	–38 36 49	250	5481	2.88	22
CD-29 2531	05 50 21.4	–29 15 21	270	5225	2.68	
CD-52 1363	05 51 01.2	–52 38 13	290	5225	2.66	53
HD 40216	05 55 43.2	–38 06 16	130	6483	3.34	33
V1358 Ori	06 19 08.1	–03 26 20	170	6178	3.26	36
CD-40 2458	06 26 06.9	–41 02 54	310	5314	2.84	12
CD-48 2324	06 28 06.1	–48 26 53	280	5383	2.85	41
TYC 4810-0181-1	06 31 55.2	–07 04 59	250	4735	2.11	125
HD 295290	06 40 22.3	–03 31 59	330	5314	2.87	39
HD 48370	06 43 01.0	–02 53 19	170	5663	2.85	9
CD-36 3202	06 52 46.7	–36 36 17	300	4917	2.41	170
HD 51797	06 56 23.5	–46 46 55	335	5390	2.95	16
HD 62237	07 42 26.6	–16 17 00	230	6127	3.37	

Table 6. The Carina association.

Ident	α(2000)	δ(2000)	$EW_{\rm Li}$ mÅ	$T_{\rm eff}$ K	$A_{\rm Li}$	$v\sin(i)$ km s^{-1}
HD 42270	05 53 29.3	–81 56 53	305	4988	2.49	30
AB Pic	06 19 12.9	–58 03 16	320	5168	2.70	12
HD 49855	06 43 46.2	–71 58 35	233	5721	3.05	12
HD 55279	07 00 30.5	–79 41 46	278	5036	2.49	9
CD-57 1709	07 21 23.7	–57 20 37	247	5225	2.63	12
CD-63 408	08 24 06.0	–63 34 03	205	5759	3.02	73
CD-61 2010	08 42 00.5	–62 18 26	275	5140	2.59	38
CD-53 1875	08 45 52.7	–53 27 28	170	5931	3.07	45
CD-75 392	08 50 05.4	–75 54 38	261	5481	2.90	44
CD-53 2515	08 51 56.4	–53 55 57	240	5607	2.97	29
TYC 8582-3040-1	08 57 45.6	–54 08 37	320	4735	2.16	24
CD-49 4008	08 57 52.2	–49 41 51	260	5567	2.98	33
CD-54 2499	08 59 28.7	–54 46 49	240	5759	3.05	128
CP-55 1885	09 00 03.4	–55 38 24	250	5645	3.03	44
CD-55 2543	09 09 29.4	–55 38 27	200	5506	2.79	15
CD-54 2644	09 13 16.9	–55 29 03	240	5607	2.97	40
V479 Car	09 23 35.0	–61 11 36	345	5012	2.58	15
HD 83096	09 31 24.9	–73 44 49	100	7116	3.57	53
HIP 46720B	09 31 25.2	–73 44 51	240	5383	2.77	
CP-52 2481	09 32 26.1	–52 37 40	245	5197	2.59	17
CP-62 1293	09 43 08.8	–63 13 04	215	5481	2.80	35
CD-54 4320	11 45 51.8	–55 20 46	190	4361	1.50	5
HD 107722	12 23 29.0	–77 40 51	80	6556	3.15	30
		Intruders				
CD-48 4797	09 33 14.3	–48 48 33	0	4226		80

Table 7. The TW Hydrae association.

Ident	α(2000)	δ(2000)	$EW_{\rm Li}$ mÅ	$T_{\rm eff}$ K	$A_{\rm Li}$	$v\sin(i)$ km s^{-1}
TWA 7	10 42 30.1	–33 40 17	530	3503	0.49	4
TWA 1	11 01 51.9	–34 42 17	435	3973	1.26	6
TWA 2	11 09 13.8	–30 01 40	535	3649	0.74	13
TWA 3B	11 10 27.8	–37 31 53	580	3321	0.31	12
TWA 3A	11 10 27.9	–37 31 52	710	3376	0.49	12
TWA 13A	11 21 17.2	–34 46 46	580	3779	1.04	12
TWA 13B	11 21 17.4	–34 46 50	550	3655	0.77	12
TWA 4	11 22 05.3	–24 46 40	380	4299	1.74	9
TWA 5A	11 31 55.3	–34 36 27	629	3533	0.63	54
TWA 5B	11 31 55.4	–34 36 29	300	3050	–0.23	16
TWA 8A	11 32 41.2	–26 51 56	600	3514	0.58	7
TWA 8B	11 32 41.2	–26 52 09	560	3240	0.21	11
TWA 26	11 39 51.1	–31 59 21	500	3050	0.03	25
TWA 9B	11 48 23.7	–37 28 48	480	3458	0.37	8
TWA 9A	11 48 24.2	–37 28 49	470	4062	1.47	11
TWA 27	12 07 33.4	–39 32 54	500	3107	0.06	13
TWA 25	12 15 30.7	–39 48 43	555	3742	0.94	13
TWA 20	12 31 38.1	–45 58 59	160	3492	–0.10	30
TWA 16	12 34 56.4	–45 38 07	360	3649	0.53	11
TWA 10	12 35 04.2	–41 36 39	500	3492	0.44	6
TWA 11B	12 36 00.6	–39 52 16	550	3592	0.65	12
TWA 11A	12 36 01.0	–39 52 10	0	9311		152

Table 8. The ϵ Chamaleontis association.

Ident	α(2000)	δ(2000)	$EW_{\rm Li}$ mÅ	$T_{\rm eff}$ K	$A_{\rm Li}$	$v\sin(i)$ km s^{-1}
EG Cha	08 36 56.2	–78 56 46	510	4268	1.86	22
η Cha	08 41 19.5	–78 57 48	0	11384		390
RS Cha	08 43 12.2	–79 04 12	0	8049		64
EQ Cha	08 47 56.8	–78 54 53	570	3529	0.57	15
CP-68 1388	10 57 49.4	–69 14 00	420	4695	2.33	26
DZ Cha	11 49 31.9	–78 51 01	560	3603	0.68	18
T Cha	11 57 13.5	–79 21 32	360	5111	2.71	39
GSC 9415-2676	11 58 26.9	–77 54 45	600	3486	0.53	5
EE Cha	11 58 35.2	–77 49 31	0	8104		93
ϵ Cha	11 59 37.6	–78 13 19	0	11384		265
HIP 58490	11 59 42.3	–76 01 26	445	4351	1.91	10
DX Cha	12 00 05.1	–78 11 35	0	7994		12
HD 104237D	12 00 08.3	–78 11 40	580	3434	0.44	6
HD 104237E	12 00 09.3	–78 11 42	480	3850	1.08	30
HD 104467	12 01 39.1	–78 59 17	260	5759	3.14	22
GSC 9420-0948	12 02 03.8	–78 53 01	540	3661	0.77	12
GSC 9416-1029	12 04 36.2	–77 31 35	470	3537	0.47	6
HD 105923	12 11 38.1	–71 10 36	280	5344	2.81	13
GSC 9239-1495	12 19 43.8	–74 03 57	560	3673	0.81	
GSC 9239-1572	12 20 21.9	–74 07 39	610	3749	1.01	41
CD-74 712	12 39 21.3	–75 02 39	459	4722	2.41	20
CD-69 1055	12 58 25.6	–70 28 49	400	4917	2.56	24
MP Mus	13 22 07.5	–69 38 12	424	4616	2.24	14

Table 9. The Octans association.

Ident	α(2000)	δ(2000)	$EW_{\rm Li}$ mÅ	$T_{\rm eff}$ K	$A_{\rm Li}$	$v\sin(i)$ km s^{-1}
CD-58 860	04 11 55.7	–58 01 47	225	5759	3.07	20
CD-43 1451	04 30 27.3	–42 48 47	280	5168	2.63	19
CD-72 248	05 06 50.6	–72 21 12	350	5059	2.58	190
HD 274576	05 28 51.4	–46 28 19	235	5683	3.03	21
CD-47 1999	05 43 32.1	–47 41 11	190	6064	3.23	39
TYC 7066-1037-1	05 58 11.8	–35 00 49	250	5383	2.79	20
CD-66 395	06 25 12.4	–66 29 10	250	5225	2.57	190
CD-30 3394A	06 40 04.9	–30 33 03	120	6490	3.30	36
CD-30 3394B	06 40 05.7	–30 33 09	170	6140	3.23	40
HD 155177	17 42 09.0	–86 08 05	80	6623	3.19	21
TYC 9300-0529-1	18 49 45.1	–71 56 58	300	5140	2.64	26
TYC 9300-0891-1	18 49 48.7	–71 57 10	310	5168	2.69	9
CP-79 1037	19 47 03.9	–78 57 43	257	5304	2.73	29
CP-82 784	19 53 56.8	–82 40 42	275	5012	2.46	39
CD-87 121	23 58 17.7	–86 26 24	266	5225	2.66	34

Table 10. The Argus association.

Ident	α(2000)	δ(2000)	$EW_{\rm Li}$ mÅ	$T_{\rm eff}$ K	$A_{\rm Li}$	$v\sin(i)$ km s^{-1}
BW Phe	00 56 55.5	–51 52 32	148	4826	1.96	28
CD-49 1902	05 49 44.8	–49 18 26	220	5645	2.96	55
CD-56 1438	06 11 53.0	–56 19 05	230	5225	2.59	130
CD-28 3434	06 49 45.4	–28 59 17	230	5607	2.95	
CD-42 2906	07 01 53.4	–42 27 56	275	5083	2.54	11
CD-48 2972	07 28 22.0	–49 08 38	250	5506	2.90	52
CD-48 3199	07 47 26.0	–49 02 51	230	5607	2.95	25
CD-43 3604	07 48 49.8	–43 27 06	320	4589	2.05	40
TYC 8561-0970-1	07 53 55.5	–57 10 07	210	5225	2.55	6
HD 67945	08 09 38.6	–20 13 50	0	7159		120
CD-58 2194	08 39 11.6	–58 34 28	270	5759	3.16	85
PMM 7422	08 28 45.6	–52 05 27	233	5683	3.02	33
PMM 7956	08 29 51.9	–51 40 40	289	4735	2.17	14
PMM 1560	08 29 52.4	–53 22 00	107	5874	2.80	6
PMM 6974	08 34 18.1	–52 15 58	74	4633	1.42	5
PMM 4280	08 34 20.5	–52 50 05	151	5759	2.87	16
PMM 6978	08 35 01.2	–52 14 01	179	4667	1.86	7
PMM 2456	08 35 43.7	–53 21 20	301	4735	2.20	48
PMM 351	08 36 24.2	–54 01 06	90	6064	2.87	90
PMM 3359	08 36 55.0	–53 08 34	226	5460	2.81	9
PMM 5376	08 37 02.3	–52 46 59	0	3999		10
PMM 4324	08 37 47.0	–52 52 12	97	6225	3.02	41
PMM 665	08 37 51.6	–53 45 46	189	5506	2.76	8
PMM 4336	08 37 55.6	–52 57 11		4964		8
PMM 4362	08 38 22.9	–52 56 48	191	5797	3.02	9
PMM 4413	08 38 55.7	–52 57 52	163	5797	2.94	9
PMM 686	08 39 22.6	–53 55 06	215	4633	1.91	13
PMM 4467	08 39 53.0	–52 57 57	190	5140	2.41	13
PMM 1083	08 40 06.2	–53 38 07	162	5988	3.09	68
PMM 8415	08 40 16.3	–52 56 29	302	5059	2.56	21
PMM 1759	08 40 18.3	–53 30 29	55	4158	0.61	4
PMM 1142	08 40 49.1	–53 37 45		5567		8
PMM 1174	08 41 22.7	–53 38 09	79	6556	3.14	60
PMM 1820	08 41 25.9	–53 22 41	333	4524	1.99	86
PMM 4636	08 41 57.8	–52 52 14	100	4139	0.86	5
PMM 3695	08 42 18.6	–53 01 57	0	3661		90
PMM 756	08 43 00.4	–53 54 08	217	5383	2.72	16
PMM 5811	08 43 17.9	–52 36 11	107	6760	3.40	59
PMM 2888	08 43 52.3	–53 14 00		6483		66
PMM 2012	08 43 59.0	–53 33 44	251	5168	2.58	17
PMM 4809	08 44 05.2	–52 53 17	175	5759	2.94	18
PMM 1373	08 44 10.2	–53 43 34	156	4785	1.94	7
PMM 5884	08 44 26.2	–52 42 32	225	5383	2.73	14
PMM 4902	08 45 26.9	–52 52 02	204	4508	1.73	8
PMM 6811	08 45 39.1	–52 26 00	137	6330	3.26	90
PMM 2182	08 45 48.0	–53 25 51	187	6094	3.24	78
CD-57 2315	08 50 08.1	–57 45 59	308	4917	2.41	24
TYC 8594-0058-1	09 02 03.9	–58 08 50	300	5432	2.93	34
CD-62 1197	09 13 30.3	–62 59 09	280	5083	2.54	84
TYC 7695-0335-1	09 28 54.1	–41 01 19	300	4735	2.19	120
HD 84075	09 36 17.8	–78 20 42	170	6216	3.28	20
TYC 9217-0641-1	09 42 47.4	–72 39 50	240	5083	2.47	23
CD-39 5883	09 47 19.9	–40 03 10	260	5225	2.65	11
HD 85151A	09 48 43.3	–44 54 08	220	5607	2.93	
HD 85151B	09 48 43.5	–44 54 09	250	5383	2.79	
CD-65 817	09 49 09.0	–65 40 21	200	5988	3.19	19
HD 309851	09 55 58.3	–67 21 22	170	6026	3.14	19
HD 310316	10 49 56.1	–69 51 22	224	5645	2.97	16
CP-69 1432	10 53 51.5	–70 02 16	195	5912	3.12	55
CD-74 673	12 20 34.4	–75 39 29	230	4616	1.92	12
CD-75 652	13 49 12.9	–75 49 48	200	5721	2.98	20
HD 129496	14 46 21.4	–67 46 16	150	6330	3.30	88
NY Aps	15 12 23.4	–75 15 16	182	5304	2.55	11
CD-52 9381	20 07 23.8	–51 47 27	60	4168	0.67	42
		Intruders				
TYC 6585-0334-1	08 56 26.3	–22 41 40	10	4226	–0.06	4

Table 11. The AB Doradus association.

Ident	α(2000)	δ(2000)	$EW_{\rm Li}$ mÅ	$T_{\rm eff}$ K	$A_{\rm Li}$	$v \sin(i)$ km s^{-1}
PW And	00 18 20.9	+30 57 22	267	4701	2.10	22
HD 4277	00 45 50.9	+54 58 40	119	6521	3.32	24
HD 6569	01 06 26.2	–14 17 47	155	5036	2.21	10
CD-12 243	01 20 32.3	–11 28 04	160	5432	2.62	3
CD-46 644	02 10 55.4	–46 03 59	250	4629	1.90	36
HD 13482	02 12 15.4	+23 57 29	145	5597	2.65	6
HIP 12635	02 42 21.0	+38 37 21	146	4917	2.05	6
HD 16760A	02 42 21.3	+38 37 07	158	5829	2.96	3
HD 17332B	02 47 27.2	+19 22 21	170	5721	2.90	8
HD 17332A	02 47 27.4	+19 22 19	155	6064	3.13	13
IS Eri	03 09 42.3	–09 34 47	191	5383	2.66	7
HIP 14807	03 11 12.3	+22 25 23	34	4226	0.49	
HIP 14809	03 11 13.8	+22 24 57	145	6102	3.13	
BD+09 412	03 12 34.3	+09 44 57	150	4735	1.86	6
V577 Per	03 33 13.5	+46 15 27	200	5729	2.99	7
HD 21845B	03 33 14.0	+46 15 19	30	3831	–0.28	20
HIP 17695	03 47 23.3	–01 58 20	0	3518		18
HD 24681	03 55 20.4	–01 43 45	230	5630	2.97	34
HD 25457	04 02 36.7	–00 16 08	100	6406	3.16	18
HD 25953	04 06 41.5	+01 41 02	120	6521	3.32	30
TYC 0091-0082-1	04 37 51.5	+05 03 08	220	5225	2.57	8
TYC 5899-0026-1	04 52 24.4	–16 49 22	20	3480	–1.09	5
CD-56 1032B	04 53 30.5	–55 51 32	0	3388		
CD-56 1032A	04 53 31.2	–55 51 37	0	3458		
HD 31652	04 57 22.3	–09 08 00	230	5460	2.82	6
CD-40 1701	05 02 30.4	–39 59 13	120	4589	1.59	7
HD 32981	05 06 27.7	–15 49 30	140	5995	3.03	6
HD 293857	05 11 09.7	–04 10 54	260	5481	2.90	11
HD 33999	05 12 35.8	–34 28 48	90	6523	3.19	7
HD 35650	05 24 30.2	–38 58 11	15	4165	0.02	4
AB DorB	05 28 44.4	–65 26 47	0	3397		
AB DorA	05 28 44.8	–65 26 56	267	5059	2.50	53
UX Col	05 28 56.5	–33 28 16	182	4491	1.65	42
CD-34 2331	05 35 04.1	–34 17 52	190	4589	1.80	25
HIP 26369	05 36 55.1	–47 57 48	70	4197	0.79	28
UY Pic	05 36 56.9	–47 57 53	285	5197	2.68	9
WX Col	05 37 12.9	–42 42 56	180	5759	2.96	6
HIP 26401B	05 37 13.2	–42 42 57	270	5012	2.45	5
Par 2752	05 38 56.6	–06 24 41	130	5607	2.68	6
CP-19 878	05 39 23.2	–19 33 29	290	5083	2.57	32
TYC 7605-1429-1	05 41 14.3	–41 17 59	250	4589	1.84	54
CD-26 2425	05 44 13.4	–26 06 15	320	4917	2.44	
TZ Col	05 52 16.0	–28 39 25	180	5988	3.15	20
TY Col	05 57 50.8	–38 04 03	210	5481	2.80	55
BD-13 1328	06 02 21.9	–13 55 33	230	4589	1.89	6
CD-34 2676	06 08 33.9	–34 02 55	240	5383	2.77	4
CD-35 2722	06 09 19.2	–35 49 31	10	3727	–0.97	13
HD 45270	06 22 30.9	–60 13 07	150	6102	3.14	18
GSC 8894-0426	06 25 56.1	–60 03 27	0	3492		
AK Pic	06 38 00.4	–61 32 00	140	6178	3.16	18
CD-61 1439	06 39 50.0	–61 28 42	40	4158	0.46	12
TYC 7627-2190-1	06 41 18.5	–38 20 36	280	4917	2.37	37
GSC 8544-1037	06 47 53.4	–57 13 32	170	4589	1.75	7
CD-57 1654	07 10 50.6	–57 36 46	180	5931	3.10	29
BD+20 1790	07 23 43.6	+20 24 59	105	4394	1.27	13
HD 59169	07 26 17.7	–49 40 51	145	5607	2.73	11
V372 Pup	07 28 51.4	–30 14 49	10	4011	–0.42	20
CD-84 80	07 30 59.5	–84 19 28	300	5196	2.70	3
HD 64982	07 45 35.6	–79 40 08	140	6330	3.27	14
BD-07 2388	08 13 51.0	–07 38 25	300	5390	2.89	130
HD 82879	09 28 21.1	–78 15 35	100	6623	3.29	140
CD-45 5772	10 07 25.2	–46 21 50	50	4589	1.18	6
BD+01 2447	10 28 55.5	+00 50 28	0	3570		0
HD 99827	11 25 17.7	–84 57 16	80	6711	3.24	45

Table 11. continued.

Ident	α(2000)	δ(2000)	$EW_{\rm Li}$ mÅ	$T_{\rm eff}$ K	$A_{\rm Li}$	$v\sin(i)$ km s^{-1}
PX Vir	13 03 49.7	–05 09 43	142	5197	2.33	6
HD 139751	15 40 28.4	–18 41 46	110	4442	1.36	8
HIP 81084	16 33 41.6	–09 33 12	0	3879		7
HD 152555	16 54 08.1	–04 20 25	133	6102	3.08	16
HD 317617	17 28 55.6	–32 43 57	120	4735	1.76	4
HD 159911	17 37 46.5	–13 14 47	250	4589	1.93	140
HD 160934	17 38 39.6	+61 14 16	40	4226	0.57	17
HD 176367	19 01 06.0	–28 42 50	140	6254	3.22	17
HD 178085	19 10 57.9	–60 16 20	165	6102	3.19	24
TYC 0486-4943-1	19 33 03.8	+03 45 40	180	4735	1.95	11
HD 189285	19 59 24.1	–04 32 06	140	5630	2.73	9
BD-03 4778	20 04 49.4	–02 39 20	290	5083	2.57	8
HD 199058	20 54 21.1	+09 02 24	160	5894	3.01	14
TYC 1090-0543-1	20 54 28.0	+09 06 07	120	4589	1.59	18
HD 201919	21 13 05.3	–17 29 13	20	4268	0.32	8
LQ Peg	21 31 01.7	+23 20 07	215	4524	1.78	66
HD 207278	21 48 48.5	–39 29 09	190	5759	2.99	10
HIP 107948	21 52 10.4	+05 37 36	0	3486		80
HIP 110526A	22 23 29.1	+32 27 34	0	3492		16
HIP 110526B	22 23 29.1	+32 27 32	0	3480		
HD 217343	23 00 19.3	–26 09 14	180	5912	3.09	12
HD 217379	23 00 28.0	–26 18 43	10	4257	–0.01	6
HIP 114066	23 06 04.8	+63 55 34	30	3879	–0.18	8
HD 218860A	23 11 52.1	–45 08 11	222	5607	2.94	7
HD 218860B	23 11 53.6	–45 08 00	0	3492		
HIP 115162	23 19 39.6	+42 15 10	160	5607	2.78	
HD 222575	23 41 54.3	–35 58 40	230	5567	2.92	31
HD 224228	23 56 10.7	–39 03 08	78	4826	1.66	3
		Intruders				
CD-41 2076	05 48 30.4	–41 27 20	20	4361	0.45	10
V402 Hya	08 53 12.1	–07 43 21	0	5111		240
CD-37 6177	09 56 58.4	–38 33 14	0	4917		
HD 110810	12 45 14.4	–57 21 29	0	4964		4